Ultrafast Studies of Excited-State Dynamics of Phthalocyanine and Zinc Phthalocyanine Tetrasulfonate in Solution

L. Howe and J. Z. Zhang*

Department of Chemistry and Biochemistry, University of California, Santa Cruz, California 95064

Received: July 24, 1996; In Final Form: December 9, 1996[⊗]

Femtosecond measurements of transient absorption, bleach, and stimulated emission are used to study the excited-state dynamics of phthalocyanine tetrasulfonate (PcS_4) and zinc phthalocyanine tetrasulfonate ($ZnPcS_4$) in solution. In water the excited-state decay process is fast and dominated by energy relaxation due to intermolecular aggregation. In dimethyl sulfoxide (DMSO) both PcS_4 and $ZnPcS_4$ exist predominantly in the monomeric form and exhibit very different dynamics from that of the aggregates. The decays are much slower and the observed processes are strongly dependent on the probe wavelength. For PcS_4 in DMSO, when probed at 790 nm, the dynamics are dominated by stimulated emission which is observed for the first time in solution. At other wavelengths either transient absorption or bleach dominates the signal. All the observed dynamics can be well fit using a double-exponential function with a fast and slow component. The fast decay has a time constant of 10 ± 4 ps for both phthalocyanines while the slow decay has a time constant of 370 ps for PcS_4 and 460 ps for $ZnPcS_4$, respectively. The overall excited-state decay dynamics correlate well with the recovery of the ground electronic state, indicating that the recovery is the predominant process on this time scale. On the basis of a simple three-state kinetic model, the fast decay (10 ps) is attributed primarily to a conversion from the second to the first excited singlet state, possibly involving vibrational relaxation in S_1. There might also be a small contribution from aggregates. The first excited-state S_1 subsequently decays with a time constant of 130 ps for PcS_4 and 160 ps for $ZnPcS_4$, respectively. This decay is due to a combination of radiative and nonradiative relaxation from S_1 to S_0 and intersystem crossing from S_1 to the triplet state.

Introduction

Phthalocyanines have been studied extensively since the first synthesis in 1907.[1] They are usually light stable and absorb readily in the red and visible regions of the spectrum. These properties have led to a wealth of interesting applications ranging from chemical sensors and nonlinear optical devices to inks, dyes, and photodynamic therapy.[2] Because of their diverse applications, the optical absorption and emission properties of these molecules in solutions have been extensively studied mainly with frequency-resolved techniques,[3] while their thin films have been investigated both spectroscopically and electrochemically.[4] The excited states of phthalocyanines are expected to play an important role in various applications, but still little is known about the excited-state dynamics of this important class of compounds on the subnanosecond time scales.[5]

Several femtosecond studies have been reported on the ultrafast excited-state dynamics of phthalocyanine films.[6,7,8,9] The excited-state dynamics of phthalocyanines are known to be sensitive to the host environment.[7] For example, exciton−exciton annihilation was found to be much more important in films than in isolated phthalocyanine molecules. However, relatively little work has been done on phthalocyanines in solutions[9−11] Understanding the excited-state dynamics of phthalocyanines in solution is vital to other applications, such as photodynamic therapy (PDT), in which a dye molecule is used for the detection and photodynamic treatment of cancer tumors.

Photodynamic therapy is an attractive way to treat cancer because of the low dark toxicity of the dye molecules and the selective localization in tumor cells. It has been a suggested treatment for many types of tumors including skin,[12] mouth, esophagus, lung, and bladder.[13] The synthesis and photoactivity of porphyrins and phthalocyanines as photosensitizers for PDT have been reviewed recently.[14,15] Despite the growing interest in photosensitizers for PDT, the only time-resolved studies of the excited-states of phthalocyanines in solutions examined the paramagnetic metallophthalocyanines (VO,[8] Ni and Co,[10] or Cu[11]). Unfortunately, the paramagnetism renders these molecules inactive as photodynamic drugs due to low singlet oxygen quantum yield, yet they are useful in other applications.

Recently, our group reported a femtosecond study of the solution dynamics of hematoporphyrin derivative (HpD),[16] the active ingredient in Photofrin II.[17] This is currently the only clinically used photodynamic cancer drug in the United States. We have found that the excited-state dynamics of HpD are very sensitive to the solvent, pH of aqueous solutions, and concentration. In particular, aggregation is found to play a dominant role in aqueous solutions.[16] Phthalocyanines have shown promise as second-generation photosensitizers, with Al and Zn(II) showing great potential.[15] The steady-state and time-gated fluorescence of zinc(II) phthalocyanine (ZnPc) encapsulated in unilamellar vesicles of dipalmitoyl phosphatidylcholine (DPPC) has been reported.[18] The results were attributed to both a monomeric (3.0−3.5 ns) and aggregated (1.2−1.4 and 0.4−0.6 ns) form. As ZnPc is hydrophobic, it can be clinically administered either enclosed in liposomes or by attaching hydrophilic groups (as is the case in $ZnPcS_4$).

In this paper we report the direct study of the excited-state dynamics of phthalocyanine tetrasulfonate (PcS_4) and zinc phthalocyanine tetrasulfonate ($ZnPcS_4$) in different solvent environments using femtosecond transient absorption spectroscopy. For both compounds the excited-state dynamics have

---

* To whom correspondence should be addressed.

[⊗] Abstract published in *Advance ACS Abstracts,* April 15, 1997.

S1089-5639(96)02244-X CCC: $14.00

been found to be sensitive to the solvent environment. In aqueous solution the excited states are short-lived and are concentration dependent, indicating that these phthalocyanines are aggregated. The process observed in water is a simple transient absorption which is independent of probe wavelength in the region observed (540−820 nm). In organic solvents such as dimethyl sulfoxide (DMSO), these molecules are mainly monomeric with longer-lived excited states, and the dynamics are more complex. In addition to transient absorption and bleach, stimulated emission of PcS$_4$ in DMSO is observed for the first time, to our best knowledge, when probed at 790 nm following excitation at 390 nm. A combination of the transient absorption, stimulated emission, and bleach provides important information for modeling the excited state of PcS$_4$. A three-state kinetic model was used to account for the dynamic features observed and to extract rate constants related to the excited-state relaxation processes. The results observed have significant implications in clinical applications of PcS$_4$ and ZnPcS$_4$ for PDT. For example, the enhanced signal from stimulated emission may prove useful in tumor imaging and PDT dosimetry.[19]

Experimental Section

Phthalocyanine tetrasulfonate (PcS$_4$) and zinc phthalocyanine tetrasulfonate (ZnPcS$_4$) were purchased from Porphyrin Products and used without further purification. Aqueous solutions were prepared with doubly distilled water to prepare solutions in the 50−170 μM range. DMSO solutions were typically 40−70 μM at the beginning of the experiment. Some sample photodegradation in DMSO was observed after long exposure to the excitation beam. Therefore, the UV−vis absorption at 390 nm was measured before and after each dynamics experiment to ensure that there was no appreciable decrease in the sample concentration. A fresh sample is used to replace the used sample when noticeable changes were observed. To further remove potential problems from photoproduct formation the number of laser pulses averaged for each data point was reduced until the scans were reproducible (200 laser pulses/point). The photoproduct formation is most likely due to reaction between the excited phthalocyanine molecule and DMSO.

The ground-state electronic absorption spectra were measured with an HP8254A diode array UV−visible spectrophotometer with 2 nm resolution. Static fluorescence spectra were obtained using a Spex Fluorolog2 spectrofluormeter (with 1 nm resolution). The fluorescence signal was detected perpendicular to the incident 390 nm excitation beam, and were corrected for background and detector wavelength sensitivity.

The transient absorption spectra of the phthalocyanine solutions were obtained using a pump−probe technique based on a regeneratively amplified, mode-locked femtosecond Ti−sapphire laser system. The details of the laser setup and the spectrometer have been described previously.[20] Pulses of 40−100 fs with 5 nJ/pulse energy and 100 MHz repetition rate were generated by a mode-locked Ti−sapphire oscillator, which were then amplified using a Quantronix regenerative amplifier pumped with a Q-switched Nd:YLF laser. Final output pulses (150 fs, 350 μJ/pulse) at 780 nm were frequency doubled in a KDP crystal to generate a 390 nm pump beam with 30 μJ/pulse with 1 kHz repetition rate. The pump power was adjusted with neutral density filters so that no solvent signal was detected, and the observed signals were linear with pump power. The remaining fundamental was focused into a quartz crystal to generate a white light continuum. An interference band path filter (10 nm fwhm) was used to select the desired probe wavelength. The pump and probe beam were delayed in time using a translation stage, and the signal was detected by a silicon photodiode. The resulting signal was normalized to a reference signal from another photodiode monitoring the laser beam.

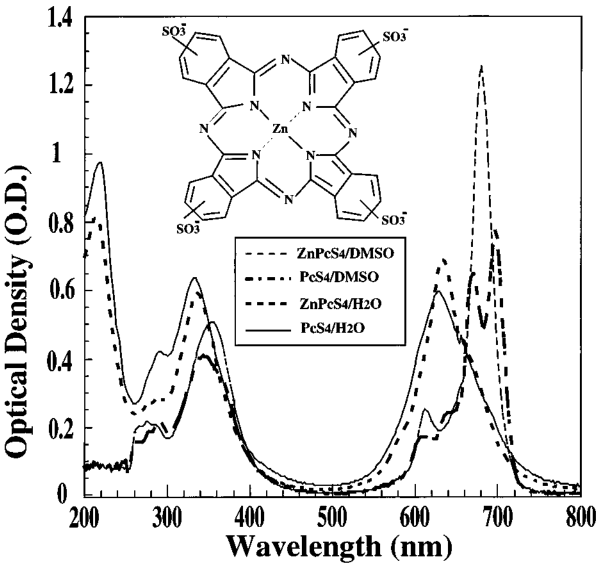

Figure 1. Electronic absorption spectra of PcS$_4$ (20 μM) and ZnPcS$_4$ (22 μM) in water and PcS$_4$ (12 μM) and ZnPcS$_4$ (8 μM) in DMSO. The spectra for the aqueous solution show the dye to be aggregated and the red-shift of the spectra in DMSO is from the monomeric form. The top insert shows the molecular structure of ZnPCS$_4$.

Results and Discussion

Static Electronic Absorption Spectra. The static electronic absorption spectra of PcS$_4$ and ZnPcS$_4$ in different solutions are shown in Figure 1. They agree well with the spectra previously reported.[3] For both phthalocyanines in water there are two strong broad bands: the Soret band ($\pi \rightarrow \pi^*$) in the near-UV ($\lambda_{\max} = 332$ and 336 nm for PcS$_4$ and ZnPcS$_4$, respectively), and the Q-band ($n \rightarrow \pi^*$) in the red ($\lambda_{\max} = 630$ nm for PcS$_4$ and 636 nm for ZnPcS$_4$). It has been observed that the low-energy Q-band shows a red-shift in organic solvents, and this has been attributed to a shift from intermolecular aggregates toward monomers.[21,22] The bands in DMSO are red-shifted and are substantially narrowed relative to the absorption bands in water, indicating that the phthalocyanines are mostly aggregated in water, while in DMSO they are monomeric. There is also an increase in the relative intensity of the Q-band in the monomeric form.

Fluorescence Spectra. The fluorescence spectra of both PcS$_4$ and ZnPcS$_4$ are shown in Figure 2. In aqueous solution the fluorescence is too weak to be detected, while in DMSO there is a strong fluorescence band in the red region (690−700 nm) and a weak band around 500 nm. The observed red fluorescence band remains the same when the excitation wavelength is changed from 390 to 670 nm, indicating that this observed red fluorescence is mainly from the first excited singlet state (S$_1$) state even when the second excited singlet state (S$_2$) state is initially populated following excitation at 390 nm. The weak blue fluorescence is probably due to emission from S$_2$ to S$_0$. This suggests that the S$_2$ state is very short-lived relative to the S$_1$ state and that the conversion from S$_2$ to S$_1$ is a rapid process. This will be discussed in more detail later.

Excited-State Dynamics in Aqueous Solution. Figure 3 shows the transient absorption profile of PcS$_4$ in aqueous solution at two different concentrations (170 and 98 μM). The molecules were excited at 390 nm and probed at 790 nm. The transient signal features a quick rise, limited by the laser pulse

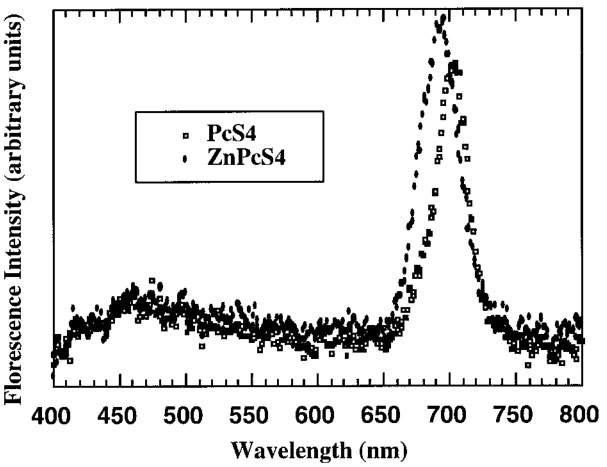

Figure 2. Fluorescence spectra of PcS_4 and $ZnPcS_4$ following excitation at 390 nm: PcS_4 in DMSO (9 μM); $ZnPcS_4$ in DMSO (7 μM). The OD at 390 nm is 0.132 for PcS_4 while the OD at 390 nm is 0.163 for $ZnPcS_4$.

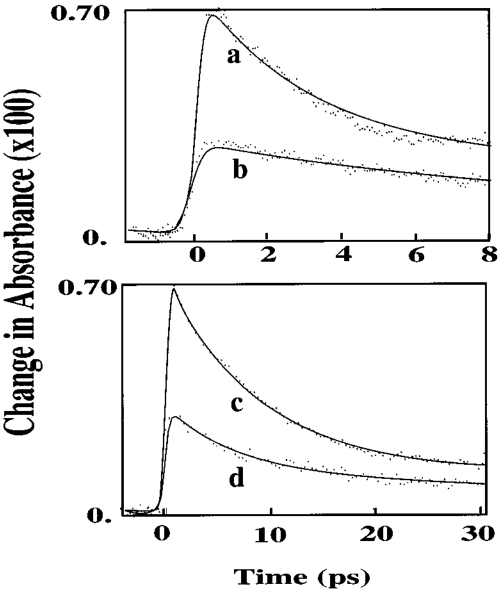

Figure 3. Transient absorption spectra of PcS_4 in water probed at 790 nm following excitation at 390 nm on two different time scales: (a) and (c) for high concentration (170 μM); (b) and (d) for low concentration (98 μM). Dotted lines are experimental data and solid lines are fits using the function discussed in the text.

(<150 fs), and a double exponential decay. The data are fit with a double-exponential function convolved with a Gaussian function (0.4 ps fwhm) representing the instrument response. The decay is faster at a higher concentration (4 and 40 ps for the high concentration, 7 and 60 ps for the low concentration). Similar results were obtained for the aqueous solution of $ZnPcS_4$. For both PcS_4 and $ZnPcS_4$ the signal shape is independent of probe wavelength in the region 540−820 nm.

Previous studies found that PcS_4 and $ZnPcS_4$ tend to form aggregates even at micromolar concentrations. The observed fast excited-state decay (<80 ps) is attributed primarily to efficient nonradiative energy relaxation due to intermolecular aggregation. This is consistent with the extremely weak fluorescence in aqueous solutions. This observation of short-lived excited-state lifetime is significant for applications in PDT since the short-lived aggregates are expected to be inefficient in singlet-state oxygen generation, which is one of the proposed mechanisms of tumor necrosis in PDT.[17] It is thus of interest to study the excited-states of monomeric phthalocyanines which are likely to be the active species for PDT and exist in organic solvents such as DMSO.

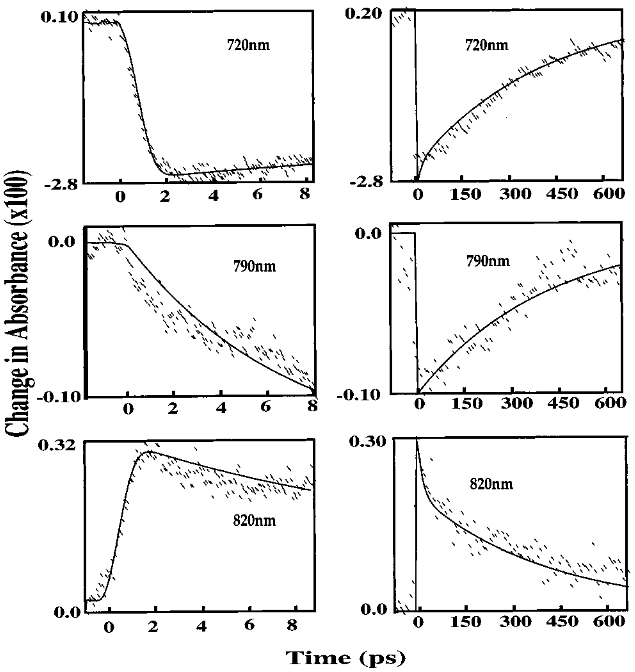

Figure 4. Transient time profile of PcS_4 in DMSO (70 μM), following excitation at 390 nm, probed at different wavelengths: 720, 790, and 820 nm.

PcS_4 in DMSO: Effect of Probe Wavelength on Observed Dynamics. In DMSO the excited-state dynamics of PcS_4 and $ZnPcS_4$ are drastically different from that in water. For both PcS_4 and $ZnPcS_4$ there is no concentration dependence in the range 10−100 μM, indicating that the observed signal is primarily due to the monomeric form. Figure 4 shows the excited-state dynamics of PcS_4 in DMSO at three representative probe wavelengths (720, 790, 820 nm) on two different time scales. Very different features are observed at these three probe wavelengths. At 720 nm, the signal is dominated by transient bleach (top panel of Figure 4) with a laser pulse-width limited decay, followed by a double-exponential rise with time constants of 10 ± 4 and 370 ± 30 ps. The PcS_4 signal has a negative amplitude and is thus clearly not transient absorption, which would be indicated by a positive signal in our data. The signal is assigned to transient bleach rather than stimulated emission for two reasons. First, at 720 nm there is a finite ground-state absorption (OD at 390 nm = 1.03, while the OD at 720 nm = 0.33 for the sample studied), a bleach signal is thus possible. Second, the fast decay is pulse-width limited, which is expected for bleach but not very likely for stimulated emission, as observed at 790 nm.

At 790 nm (middle panel of Figure 4), the signal is also negative and features an initial decay with a time constant of 8 ps and a slow rise of 370 ps. The signal is again the opposite of a normal transient absorption signal and is thus due to either bleach or stimulated emission. The signal is attributed to stimulated emission of PcS_4 rather than bleach for two reasons. First, the ground state of PcS_4 does not absorb at 790 nm, and thus no bleach signal from the ground state is possible. Second, the finite initial decay time of 8 ps is apparently not limited by the laser pulse. A pulse-width limited decay would be expected for a bleach signal, as observed at 720 nm. The observed stimulated emission at 790 nm is attributed to a radiative transition from the S_1 to the ground S_0 state rather than from the S_2 to S_1 state. This is not only consistent with the observed

TABLE 1: Summary of Fitting Parameters of Excited State Dynamics

compound	probe wavelength (nm)	process	τ_1 (ps)	τ_2 (ps)
$ZnPcS_4$	720	bleach	10 ± 4	460 ± 30
$ZnPcS_4$	760	no signal		
$ZnPcS_4$	790	TA[a]	10 ± 4	460 ± 30
$ZnPcS_4$	820	TA	10 ± 4	460 ± 30
PcS_4	720	bleach	10 ± 4	370 ± 30
PcS_4	760	very small TA signal		
PcS_4	790	SE[b]	8 ± 3	370 ± 30
PcS_4	820	TA	10 ± 4	370 ± 30

[a] TA for transient absorption. [b] SE for stimulated emission.

fluorescence signal but also supported by the three-state kinetic model to be discussed later.

At 820 nm (bottom panel of Figure 4), a normal transient absorption is observed. The signal shows a quick rise and double-exponential decay. The rise is clearly pulse-width limited, and the double-exponential decay has a time constant of 10 and 370 ps. It is interesting to notice that the signals at 820 nm and the bleach signal at 720 nm are superimposable through a mirror reflection with respect to the baseline. The transient absorption signal has been found to contain contributions from both the S_2 and S_1 states; the fast decay reflects primarily the conversion of PcS_4 from S_2 to S_1, while the slow decay is mainly due to conversion from S_1 to S_0, as explained in more detail using a three-state kinetic model later. This observation strongly indicates that the excited-state decay leads primarily to recovery of the ground state.

The transient bleach signal observed at 720 nm can also provide an upper bound for the quantum yield of the triplet state, following excitation at 390 nm, which is an important piece of information for singlet oxygen generation and thus for PDT. From the top panel of Figure 4, it can be seen that approximately 60% of the initially photoexcited molecules relax back to the ground electronic state within 370 ps. This suggests that the triplet state yield must be less than 40%. Others have reported group three metal phthalocyanines with triplet quantum yields of 0.4, 0.7, and 0.9 for chloroaluminum, chlorogalium, and chlorindium phthalocyanines in 1-chloronapthalene, respectively.[23] This estimate is based on the assumption that there is no (or negligible) contribution to the ground-state recovery from the triplet-state decay due to reaction with the ground triplet state of oxygen. This assumption is reasonable considering that the triplet-state lifetime and the time scale for reaction between the triplet state phthalocyanine and triplet state oxygen are expected to be much longer than 370 ps. In aqueous solutions, the singlet oxygen quantum yield of PcS_4 is 0.14 (excitation $\lambda = 670$ nm), while for $ZnPcS_4$ the quantum yield of 0.24 (excitation $\lambda = 550$ nm) to 0.45 (excitation $\lambda = 670$ nm) has been reported.[24] With the exception of the stimulated emission at 790 nm, all the observed wavelengths (transient absorption or bleach) are fit with a double-exponential decay or rise. The fitting time constants are summarized in Table 1. The fast 10 ± 4 ps component is attributed primarily to a conversion from the $S_2 \rightarrow S_1$ state rather than vibrational relaxation, because this fast component is independent of probe wavelength. The slower component of 370 ps is mainly due to relaxation from S_1 to the ground-state S_0. This suggests that S_1 plays an important role in the excited-state dynamics of PcS_4 in solution even when S_2 is initially excited at 390 nm.

ZnPcS4 in DMSO: Effect of Probe Wavelength on Observed Dynamics. Figure 5 shows the transient time profile for $ZnPcS_4$ for the same set of probe wavelengths used for PcS_4. The dynamic features observed for $ZnPcS_4$ are very different from those for PcS_4. At both 820 and 790 nm (middle and bottom panels of Figure 5) the transient signals show a laser pulse-width limited rise and double-exponential decay with time constants of 10 ± 4 and 460 ± 30 ps, respectively. The positive signals indicate that they are dominated by transient absorption. At a bluer wavelength, e.g., 760 nm, there is no observable signal for $ZnPcS_4$ (for PcS_4 a small transient absorption was observed at 760 nm). This is most likely due to a coincidental cancellation between bleach and transient absorption at this wavelength.

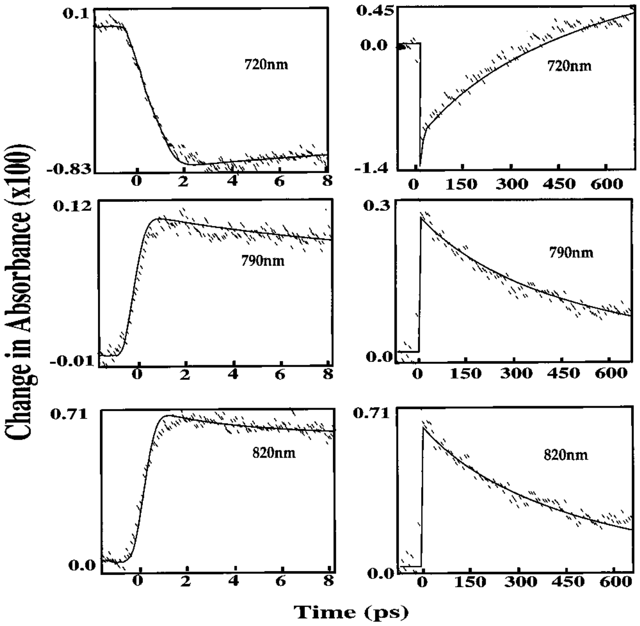

Figure 5. Same spectra as Figure 4 except with $ZnPcS_4$ (40 μM).

At even bluer wavelengths such as 720 nm (top panel of Figure 5), the observed signal becomes negative at short times and shows a quick initial decay followed by a double-exponential rise with time constants of 10 and 460 ps. For reasons similar to that used above for PcS_4, this $ZnPcS_4$ signal is attributed to a bleaching of the ground state. This bleaching signal dominates at short times and at longer times the signal recovers via a double exponential.

It is particularly interesting to note that the recovery goes beyond the baseline at longer times. The signal above the baseline is completely reproducible and is clearly due to transient absorption. It is observed that the amplitude ratio between transient bleach and transient absorption changes as a function of concentration and excitation intensity. These features are observed only for $ZnPcS_4$ when probed at 720 nm, indicating that a different process is being observed here. The reason for this will be explained in more detail next. Again, the fast component of the decay (10 ps) is attributed to conversion from S_2 to S_1 while the slower decay component (460 ps) is assigned to decay of S_1 into S_0. It is interesting to notice that the presence of Zn in $ZnPcS_4$ appears to increase the lifetime of the S_1 state (460 ps) relative to PcS_4 (370 ps).

The seemingly anomalous behavior observed for $ZnPcS_4$ at 720 nm is worth some discussion. As stated earlier, at other probe wavelengths the same double exponential decay is observed for both the transient absorption and the bleach (10 and 460 ps for $ZnPcS_4$). It is clear that both the bleach and transient absorption contribute to the signal at 720 nm. The signal is initially dominated by bleach, which is consistent with the reasonably strong ground-state absorption at 720 nm. This

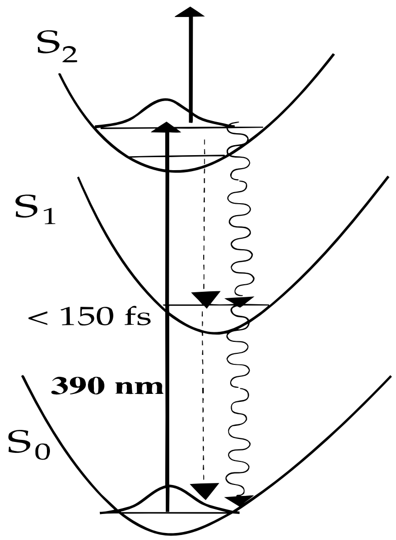

Figure 6. Schematic energy level diagram for the ground electronic state, S_0, and first two singlet excited electronic states, S_1 and S_2, of phthalocyanines.

bleaching signal size is dependent on the concentration or the OD at 720 nm. At low concentrations the Q-band is weak, the OD at 720 nm is close to zero, and there is little bleaching. At higher concentrations the Q-band is stronger and the OD at 720 nm increases so that bleaching becomes significant. At longer time, transient absorption becomes more dominant and results in a signal going above the baseline (positive). The amplitude of the bleach component appears to be linearly proportional to the excitation intensity while the transient absorption component does not seem to be sensitive to the excitation intensity. This indicates a nonlinear process, e.g., saturation, in $ZnPcS_4$ at this wavelength. Similar nonlinear or saturable absorption processes have been observed in phthalocyanines previously and have been explained by a reverse saturable absorber model.[25,26] Reverse saturable absorption is observed when a transition takes place from a ground state with a small absorption cross section to an excited-state with a larger absorption cross section. This optical limiting response has been shown to be enhanced with heavy metals[26c] which is consistent with our results on $ZnPcS_4$. The 720 data observed can be modeled as a combination of a bleach signal and an absorption signal. We can fit the data observed as a function of concentration or excitation intensity by adjusting the relative contributions of the two components, as explained in the kinetic model next. The nonlinear dependence of the transient absorption component on excitation intensity is attributed to a higher absorption cross section of the S_1 state than the S_0 state. In this case the S_0 bleach depends linearly on excitation intensity while the transient absorption is essentially independent of the excitation intensity since the S_1 state cross section is larger than the S_0 state and is saturated. In other words, at 720 nm the transient absorption from S_1 saturates more easily than the absorption from S_0.

A Kinetic Model of the Excited States. The observations described in the previous sections led us to propose the following model for the excited-state kinetics of PcS_4 and $ZnPcS_4$. As shown in Figure 6, photoexcitation at 390 nm initially populates the second excited electronic state, S_2, which occurs within the laser pulse (<150 fs). At the same time, this excitation creates a bleaching of the ground electronic state, S_0. The second laser pulse used to probe the excited molecule can, in principle, be absorbed by molecules in any one of three states: S_0, S_1, or S_2, depending on their absorption cross section at the probe wavelength (we have assumed the triplet absorption is negligible). For the data presented, transient absorption, transient bleach, as well as stimulated emission have been observed, and their contributions to the overall observed signal depend on the relative absorption cross sections at the specific probe wavelength used and the population of the different states involved. In general, we have found that transient absorption signals come from both the S_2 and S_1 state. Stimulated emission observed in PcS_4 at 790 nm is mainly from the S_1 state. The transient bleach signal is due to ground state absorption and provides important information about the recovery time of the photoexcited molecules.

TABLE 2: Summary of Rate Constants and Resulting Time Constants for Kinetic Model

compound	probe λ (nm)	process	% of $S_0/S_1/S_2$[a]	τ_1^M (ps)	τ_3M (ps)
$ZnPcS_4$	720	bleach	80/10/10	10 ± 4	160 ± 30
$ZnPcS_4$	760	no signal			
$ZnPcS_4$	790	TA	0/40/60	10 ± 4	160 ± 30
$ZnPcS_4$	820	TA	0/40/60	10 ± 4	160 ± 30
with $k_1 = k_2 = 0.1$ ps^{-1} and $k_3 = 6.3 \times 10^{-3}$ ps^{-1}					
PcS_4	720	bleach	80/20/0	10 ± 4	130 ± 30
PcS_4	760	small TA	0/40/60		
PcS_4	790	SE	0/100/0	8 ± 3	130 ± 30
PcS_4	820	TA	0/30/70	10 ± 4	130 ± 30
with $k_1 = k_2 = 0.1$ ps^{-1} and $k_3 = 7.7 \times 10^{-3}$ ps^{-1}					

[a] Relative contribution from S_0, S_1, and S_2.

To gain further insight into the energy relaxation mechanism in PcS_4 and $ZnPcS_4$, we have used a simple three-state kinetic scheme to model the observed dynamics. This model is clearly not unique but provides a consistent description of all the key dynamic features observed. The scheme is based on fast equilibration between S_2 and S_1 and relatively slow decay of S_1 back to S_0.

$$S_2 \underset{k_2}{\overset{k_1}{\rightleftarrows}} S_1 \xrightarrow{k_3} S_0 \qquad (1)$$

When $k_1 = k_2 \gg k_3$, the above scheme leads to a double-exponential decay of S_2, a fast exponential rise followed by a slow exponential decay of S_1, and a double-exponential rise of S_0. By combining different contributions from the three states, we are able to fit the data for all probe wavelengths and a specific set of rate constants which are summarized in Table 2. As an example, for $k_1 = k_2 = 0.1$ ps^{-1} and $k_3 = 7.7 \times 10^{-3}$ ps^{-1}, curves can be generated to fit the dynamics data for PcS_4, which are dominated by transient absorption, stimulated emission or transient bleach, as shown in Figure 7. For the bleach data at 720 nm, the signal is dominated (80%) by contribution from the ground state, S_0, but there is substantial contribution from the S_1 state (20%). For the 820 nm transient absorption data, the signal is dominated by the S_2 state (70%) with some (30%) contribution from the S_1 state. For the 790 nm data (the stimulated emission of PcS_4) the signal is dominated by the S_1 state. The laser pulse-width limited rise or decay is not fit since no convolution is used in this kinetic model. However, there is very little difference on the time constants of the double exponential even when convolution is used, since the time constants (10 ps and 460 or 370 ps) are much longer than the instrument response time (<0.4 ps).

The model works equally well for both $ZnPcS_4$ and PcS_4. For $ZnPcS_4$, $k_1 = k_2 = 0.1$ ps^{-1} and $k_3 = 6.3 \times 10^{-3}$ ps^{-1} are found to give the best fit to the data (not shown). Given that the model is relatively simple with only three rate constants, the agreement between the modeled curves and experimental data is very good (Figure 7). The kinetic rate constants used to model the data give time constants for the conversion between different electronic states. For instance, the S_1 to S_0 conversion

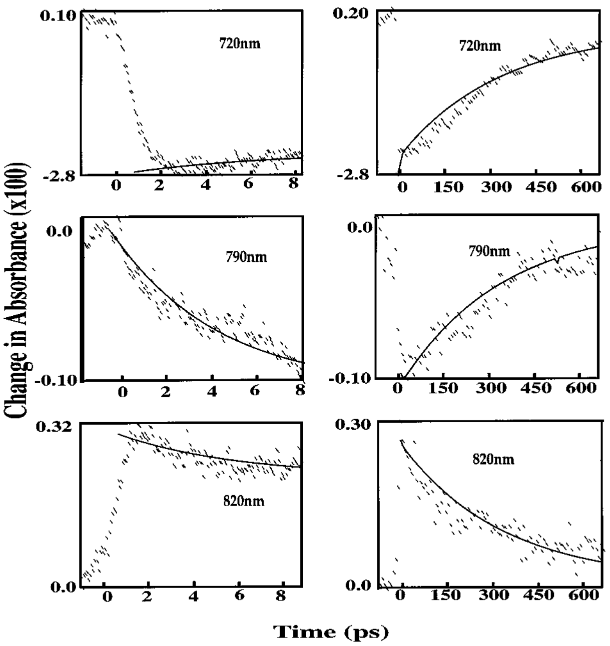

Figure 7. Comparison between experimental data (dotted lines) of PcS_4 and fitting curves (solid lines) generated by combination different contributions from the three states, S_2, S_1, and S_0, using a three-state kinetic model. See text for more details.

has a time constant ($\tau_3{}^M = 1/k_3$) of 130 ± 30 ps for PcS_4 and 160 ± 30 for $ZnPcS_4$, while the interconversion between S_2 and S_1 has a time constant ($\tau_1{}^M = 1/k_1$) of 10 ± 4 ps for both PcS_4 and $ZnPcS_4$. This model has helped to provide further physical insight into the excited-state dynamics of PcS_4 and $ZnPcS_4$. Note these time constants derived from modeling are not to be confused with those obtained from simply fitting the data with exponential functions (τ_1 and τ_2 in Table 1).

Two comments are in order on the time or rate constants obtained from the above modeling of the data. First, the fast time constant of 10 ps for both PcS_4 and $ZnPcS_4$ has been attributed primarily to conversion from S_2 to S_1. Vibrational relaxation in the S_1 state is also possibly contributing to this decay process. It is difficult to distinguish between the electronic conversion and vibrational relaxation on this fast time scale. This decay has been treated as one single step in the simple kinetic model. However, the lack of a probe wavelength dependence of this time constant seems to indicate that vibrational relaxation is not the rate-limiting step, since vibrational relaxation is usually accompanied by a blue-shift of the transient absorption spectrum and thus a probe wavelength dependence of the time constant. There is also a possibility that there is still a small contribution from aggregates even in DMSO, and this could contribute to the fast decay component. Second, the slow decay, 130 ± 30 ps for PcS_4 and 160 ± 30 ps for $ZnPcS_4$, has been attributed to conversion from S_1 to S_0. This rate constant associated with this decay time has three contributions: radiative decay from S_1 to S_0, nonradiative decay from S_1 to S_0, and intersystem crossing from S_1 to the triplet state. The contribution from the radiative decay from S_1 to S_0 is expected to be small since the radiative decay lifetime is expected to be long (a few nanoseconds), except in the case of stimulated emission. It is not possible from the data we have to separate the two contributions from nonradiative decay from S_1 to S_0 and intersystem crossing from S_1 to the triplet state. The intersystem crossing is thus not explicitly treated in the model and not included in Figure 6. It is clear, however, that intersystem crossing will contribute to the decay rate of S_1 as well as the recovery rate of S_0 since it is known that the triplet state is formed with a significant fraction.

Conclusion

The excited-state dynamics of PcS_4 and $ZnPcS_4$ have been investigated in both aqueous and organic solutions using femtosecond laser spectroscopy. The dynamics in aqueous solution are dominated by aggregates, which have short lifetimes (<80 ps). In the organic solvent DMSO, these phthalocyanines exist primarily in the monomeric form, and the excited-states are much longer lived. The longer lifetime is more favorable for generation of the triplet-state and thus singlet-state oxygen. Under physiological conditions monomers are expected to be the active component for PDT. Since the physiological environment is usually aqueous, the formation of monomers from aggregates is necessary, which is most likely facilitated by the biological substrate. Disaggregation on biological tissues is one possible mechanism, as has been suggested before for other photodynamic drugs such as HpD.[20,27] Recently, it has been shown that there is a red-shift in the absorption and emission spectra of disulfonated aluminum phthalocyanine ($AlPcS_2$) in the presence of human serum albumin (HSA), which is consistent with the formation of monomers.[28] Preliminary results obtained in our lab using PcS_4 and $ZnPcS_4$ in aqueous solutions of HSA also indicate disaggregation of the phthalocyanines. Further investigation of the interaction of phthalocyanines with biological substrates is clearly necessary, especially using time-resolved techniques. The observation of stimulated emissions in PcS_4 in DMSO at 790 nm is interesting in that it may have useful applications in the diagnosis and detection of cancer tumors and in electrooptical applications. $ZnPcS_4$ has also been shown to behave as an optical reverse saturable absorber in the first excited state at 720 nm, which may find use as a saturable absorber in the development of dye or solid-state lasers, as phthalocyanines have been used before for passive Q-switch devices.[26b]

Acknowledgment. The authors would like to acknowledge the Petroleum Research Fund administered by the American Chemical Society and University of California at Santa Cruz for financial support of this project.

References and Notes

(1) *The Phthalocyanines*; Vol I-II, Moser, F. H., Thomas, A. L., Eds.; CRC Press: Boca Raton, FL, 1983.

(2) Ben-Hur, E.; Rosenthal, I. *Int. J. Radiat. Biol.* **1985**, *47*, 145.

(3) *Phthalocyanines: Properties and Applications*; Leznoff, C. C., Lever, A. B. P., Eds.; VCH Publishers: New York, 1989; p 262.

(4) Mukhopadhyay, S.; Hogarth, C. A. *Adv. Mater.* **1994**, *6*, 162. (b) Mukhopadhyay, S.; Ray, A. K. *Int. J. Electron.* **1992**, *73*, 1055. (c) Jardin, C.; Gergely, G.; Gruzza, B. *Mater. Chem. Phys.* **1992**, *32*, 197. (d) Wilson, A.; Wright, J. D. *Mol. Cryst. Liq. Cryst.* **1992**, *211*, 321.

(5) Butvilas, V.; Gulbinas, V.; Urbas, A. *Ultrafast Processes Spectrosc.* **1991**, *6*, 499.

(6) Williams, V. S.; Mazumdar, S.; Armstrong, N. R.; Ho, Z. Z.; Peyghambarian, N. *J. Phys. Chem.* **1992**, *96*, 4500.

(7) Terasaki, A.; Hosoda, M.; Wada, T.; Tada, H.; Koma, A.; Yamada, A.; Sasabe, H.; Garito, A. F.; Kobayashi, T. *J. Phys. Chem.* **1992**, *96*, 1034.

(8) Gulbinas, V.; Chachisvilis, M..; Valkunas, L.; Sundström, V. *J. Phys. Chem.* **1996,** *100*, 2213.

(9) Asahi, T.; Tamai, N.; Uchida, T.; Shimo, N.; Masuhara, H. *Chem. Phys. Lett.* **1995**, *234*, 337.

(10) Millard, R. R.; Greene, B. I. *J. Phys. Chem.* **1985**, *89*, 2976.

(11) Kirk, A. D.; Langford, C. H.; Saint Joly, C.; Lesage, R.; Sharma, D. K. *J. Chem. Soc., Chem. Commun.* **1984**, 961.

(12) Agarwal, R.; Athar, M.; Elmets, C. A.; Bickers, D. R.; Mukhtar, H. *Photochem. Photobiol.* **1992**, *56*, 43.

(13) Van den Bergh, H. *Hadrontherapy Oncol.* **1994**, 577.

(14) (a) Bensasson, R. V.; Land, E. J.; Truscott, T. G. *Excited States and Free Radicals in Biology and Medicine*; Oxford University Press: New York, 1993; p 322. (b) *Photosensitizing Compounds: Their Chemistry,*

Biology and Clinical Use; Dougherty, T. J., Chairman; Ciba Foundation Symposium 146; John Wiley & Sons: Chichester, UK, 1993.

(15) Bonnett, R. *Chem. Soc. Rev.* **1995**, *24*, 19.

(16) Zhang, J. Z.; O'Neil, R. H; Evans, J. E. *Photochem. Photobiol.* **1994**, *60*, 301.

(17) (a) Doughtery, T. J. *Photochem. Photobiol.* **1987**, *45*, 879. (b) Agarwal, R.; Athar, M.; Elmets, C. A.; Bickers, D. R.; Mukhtar, H. *Photochem. Photobiol.* **1992**, *56*, 43. (c) Keene, J. P.; Kessel, D. E.; Land, J. R.; Redmond, W.; Truscoutt, T. G. *Photochem. Photobiol.* **1986**, *43*, 117. (d) Bohm, F.; Marston, G.; Truscott, T. G.; Wayne, R. P. *J. Chem. Soc., Faraday Trans.* **1994**, *90*, 2453. (e) Rosenthal, I.; Krishna, C. M.; Riesz, P.; Ben-Hur, E. *Radiat. Res.* **1986**, *107*, 136.

(18) Valduga, G.; Reddi, E.; Jori, G. *J. Photochem. Photobiol. B: Biol.* **1992**, *16*, 331.

(19) Moan, J.; Anholt, H. *Photochem. Photobiol.* **1990**, *51*, 379.

(20) Zhang, J. Z.; O'Neil, R. H.; Roberti, T. W. *J. Phys. Chem.* **1994**, *98*, 3859.

(21) Harriman, A.; Richoux, M. *J. Photochem.* **1980**, *14*, 253.

(22) Oddos-Marcel, L.; Madeore, F.; Bock, A.; Neher, D.; Ferencz, A.; Rengel, H.; Wegner, G.; Kryschi, C.; Trommsdorff, H. P. *J. Phys. Chem.* **1996**, *100*, 11850.

(23) Brannon, J. H.; Magde, D. *J. Am. Chem. Soc.* **1980**, 102:1, 62.

(24) Rosenthal, I.; Murali Krishna, C.; Riesz, P.; Ben-Hur, E. *Radiat. Res.* **1986**, *107*, 136.

(25) McCahon, S. W.; Tutt, L. W.; Klein, M. B.; Valley, G. C. *Proc. SPIE* **1990**, *1307*, 304.

(26) Coulter, D. R.; Miskowski, V. M.; Perry, J. W.; Wei, T.; Van Stryland, E. W.; Hagan, D. J. *Proc. SPIE* **1989**, *1105*, 42. (b)Wei, T.; Hagan, D. J.; Sence, M. J.; Van Stryland, E. W.; Perry, J. W.; Coulter, D. R. *Appl. Phys. B* **1992**, *54*, 46. (c) Perry, J. W.; Mansour, K.; Marder, S. R.; Perry, K. J.; Alvarez, Jr., D.; Choong, I. *Opt. Lett.* **1994**, *19*, 625.

(27) Liu, W.; Ramponi, R.; Cubeddu, R.; Lui, S. *Chin. Sci. Bull.* **1990**, *35*, 321.

(28) Abroz, M.; MacRobert, A. J.; Morgan, J.; Rumbles, G.; Foley, M. S.; Phillips, D. *Photochem. Photobiol. B: Biol.* **1994**, *22*, 105.